PROCEEDINGS OF SCIENCE

Lighting up the sky : What gamma rays reveal about supernova remnant shocks (and shocks in general)

Marianne Lemoine-Goumard[a,*]

[a] *Université Bordeaux, CNRS, LP2I Bordeaux, UMR 5797, F-33170 Gradignan, France*

E-mail: lemoine@lp2ib.in2p3.fr

Gamma-ray observations over the past decade—from space-based instruments like *Fermi*-LAT to ground-based arrays such as H.E.S.S., MAGIC, and VERITAS—have provided an increasingly detailed view of supernova remnants (SNRs). Several dozens of SNRs have been detected in the GeV–TeV energy range, revealing a diverse population shaped by their environments and evolutionary stages, and new detections continue to expand the catalog of gamma-ray bright remnants. Observations by HAWC and LHAASO have even identified a few Galactic PeVatron candidates, though a direct connection to SNRs remains under investigation. Beyond remnants, gamma-ray detections from novae also underscore the ubiquity of shock-powered emission across explosive astrophysical systems. This review will highlight recent gamma-ray results offering fresh insight into the radiative signatures and energetic processes associated with supernova remnant shocks.

39th International Cosmic Ray Conference (ICRC2025)
15–24 July 2025
Geneva, Switzerland

ICRC 2025
The Astroparticle Physics Conference
Geneva July 15-24, 2025

*Speaker

PoS(ICRC2025)1403

1. Introduction to gamma-ray instruments and particle acceleration

1.1 Complementarity of gamma-ray instruments

Gamma-ray astronomy employs a diverse array of instruments, each with unique capabilities, to study supernova remnants (SNRs) across different energy regimes. Space-based observatories like *Fermi*-LAT offer full-sky coverage with a large field of view (20% of the sky) and sensitivity in the GeV energy range ($\sim$ 50 MeV to 300 GeV). This extensive coverage is ideal for detecting and monitoring transient and diffuse sources, including radio-dim SNRs that might be overlooked in other wavelengths. Ground-based particle detectors such as LHAASO, HAWC, and Tibet ASγ provide large field-of-view ($\sim$ 1 steradian) and high duty cycle observations, crucial for surveying the sky for extended sources and transient events. However, these instruments typically offer lower angular resolution compared to Cherenkov telescopes, making them more suitable for detecting diffuse emission regions and large-scale structures. In contrast, Cherenkov telescopes like H.E.S.S., VERITAS, MAGIC and the upcoming CTA Observatory (CTAO) deliver excellent angular ($< 0.1^\circ$) and energy resolution in the TeV regime ($\sim$ 100 GeV to 100 TeV). Traditionally, their smaller field of view and lower duty cycle limited their ability to survey the entire sky, but this limitation will be mitigated with CTAO, where the Medium-Sized Telescopes (MSTs) and Small-Sized Telescopes (SSTs) have larger fields of view, allowing for more efficient coverage of extended Galactic sources. These instruments are pivotal for resolving fine structures within SNRs and constraining the origin of the gamma-ray emission.
The complementary nature of these instruments allows for a holistic approach to studying SNRs. Space-based observatories provide broad coverage and sensitivity to transient events and large-scale structures, ground-based particle detectors capture extended sources and high-energy phenomena, and Cherenkov telescopes supply high-resolution imaging critical for disentangling emission mechanisms. Together, they enable a comprehensive mapping of the Galactic SNR population, shedding light on CR (cosmic-ray) acceleration and the evolution of the interstellar medium.

This review explores the full life cycle of shocks revealed by gamma-ray observations, from the very early phases of core-collapse supernovae and novae, through historical remnants, to evolved supernova remnants interacting with molecular clouds. Together, these observations provide a global picture of how shocks drive particle acceleration across different stages of stellar explosions and different environments, allowing to shed new light on the long-standing PeVatron puzzle, i.e. which are the sources in our Galaxy accelerating CRs up to the knee of the CR spectrum.

1.2 Particle acceleration and shocks

The gravitational collapse of the core of a massive star into a neutron star [1] releases sufficient energy to drive a supernova explosion. The resulting blast wave expands into the circumstellar medium (CSM) and the interstellar medium (ISM), sweeping up ambient material into a hot, compressed shell. As the shock front decelerates due to the accumulating mass, a reverse shock propagates inward through the ejecta. In addition to heating the swept-up gas, a fraction of the shock energy is transferred into relativistic particles via diffusive shock acceleration (DSA) [2]. In this process, energetic particles escaping upstream from the shock excite turbulence, which in turn scatters other particles back toward the shock, enabling multiple shock crossings and efficient

acceleration. The maximum energy of this population of non-thermal particles is limited by radiative losses, the age of the SNR, or particle escape. Such particle acceleration by SNR shocks has long been suggested as a process by which cosmic rays are produced since only $\sim$ 10% of the SNR kinetic energy channeled into accelerated particles would provide sufficient energetics to reproduce the CR flux observed at Earth (see [4] for a complete review on cosmic-ray acceleration). However, it remains unclear whether they can accelerate particles to PeV energies, particularly after the very early stages of their evolution. Diesing et al. (2023) [6] have used a multi-zone, semi-analytic acceleration framework, informed by kinetic simulations, to constrain the maximum energy across a broad range of astrophysical shocks. Their analysis shows that SNRs can accelerate protons to PeV energies only under specific conditions, namely when shock velocities exceed 10^4 km/s and escaping particles drive efficient magnetic-field amplification. Even then, SNRs will only produce PeV particles for a brief period at roughly t $\sim$ 100 years for the uniform case and prior to t $\sim$ 100 years for the wind case as can be seen in Figure 1 (left). The same conclusion was reached independently by Cristofari et al. (2020) [5], i.e. only the remnants of very powerful, rare core-collapse supernova explosions can accelerate light elements such as hydrogen and helium nuclei, to the knee rigidity. The authors also confirm that standard thermonuclear explosions leading to type Ia supernovae are limited to accelerating cosmic rays up to energies of $\leq$ 100 TeV, as one can see in Figure 1 (right).

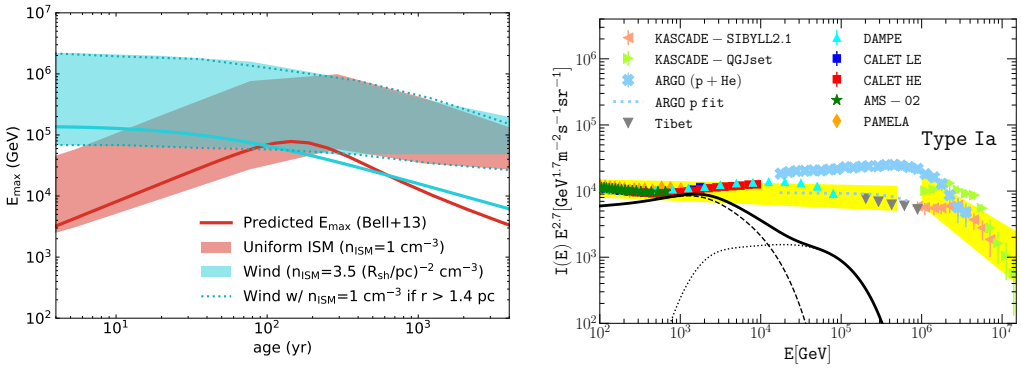

Figure 1: Left: The maximum energy, Emax, accelerated by SNR as a function of time, expanding into a uniform medium (red band) and wind profile (blue band), from [6]. The widths of the bands correspond to uncertainties in the nature of CR-driven magnetic field amplification (i.e., the lower (upper) limit assumes diffusing (escaping) particles drive amplification). Blue dotted lines indicate how the wind prediction would change if that wind had a finite size of 1.4 pc, corresponding to a shock age of $\sim$ 200 yr. Solid lines give the single-zone Emax prediction put forth in [3]. Right: Galactic CR protons from type Ia SNRs from [5]. Contributions from cumulative accelerated particles $N_{\rm acc}$ (dashed), escaping particles $N_{\rm esc}$ (dotted) and their sum (solid) are shown.

2. Fast shocks in young core-collapse supernovae and novae

2.1 Gamma-ray emission from young core-collapse supernovae

Due to these constraints, searching for gamma-ray emission at a very early expansion stage, when the forward shock is interacting with a very dense CSM, may lead to interesting prospects.

This is the case for core-collapse SNe, which evolve in the winds of their progenitor stars. Due to CR driven instabilities, the magnetic field at the shock can be amplified by factors of several hundreds allowing to further accelerate particles to very high energies. For a constant mass-loss rate and wind velocity, the density of the surrounding CSM decreases as R^{-2}, and is thus highest at radii close to the star. Hadronic emission is therefore expected to be the highest close to the star. The maximum CR (hadrons) energy is fixed by five different processes: the shock age limitation, the finite spatial extend of the shock, the generated current limitation, the nuclear interaction losses, and the adiabatic losses. The study carried by Marcowith et al. (2018) [7] shows that particles can be accelerated up to 1 PeV in such conditions which offers very good prospects for TeV instruments though absorption can be an issue at those energies.
And indeed, some interesting results have been recently posted on superluminous supernovae. These superluminous SNe have luminosities 10 to 100 times larger than usual core-collapse SNe. The energy sources of these energetic explosions are still in debate and the widely discussed scenarios include ^{56}Ni decay, the interaction between ejecta and dense circumstellar media and the spin-down of the nascent magnetar. Dedicated efforts to search for gamma-ray emission from SLSNe with the Fermi Large Area Telescope (*Fermi*-LAT) have been performed without any success until the very recent publication by Li et al. (2024) [12] announcing the detection of a transient γ-ray source appearing nearly 2 months after the explosion of SN 2017egm and lasting a few months. Both the peak time and the luminosity of the GeV emission are consistent with the magnetar model prediction, suggesting that such a GeV transient is the high-energy counterpart of SN 2017egm and the central engine of this SLSNe is a young magnetar. F. Acero and collaborators have performed a dedicated analysis confirming this detection [13].

2.2 Gamma-ray emission from novae: fast shocks as real-time particle accelerators

Gamma-ray emission from novae, particularly in the TeV range, has emerged as a significant avenue for studying particle acceleration in astrophysical environments. Novae are explosive events that occur in binary systems when a white dwarf accretes material from a companion star. Two main types are distinguished: classical novae, involving a white dwarf accreting from a main-sequence or subgiant star, and symbiotic novae, where the companion is an evolved red giant with a dense stellar wind. Both types have been detected in the GeV range with *Fermi*-LAT, demonstrating that efficient particle acceleration is a generic feature of nova outbursts. The symbiotic nova RS Ophiuchi, during its 2021 outburst, became the first nova to be detected in the very-high-energy (VHE) gamma-ray domain, with observations by H.E.S.S. [8], MAGIC [9] and LST-1 [10] revealing transient gamma-ray emission up to $\sim$ 10 TeV. This emission is attributed to particle acceleration at shocks formed when the nova ejecta collide with the dense wind from its red giant companion. The temporal profile of the gamma-ray emission, characterized by a rapid rise and a power-law decay, supports the external shock scenario. Notably, the TeV gamma-ray peak occurred approximately two days after the GeV peak, suggesting a complex shock structure or temporal delay to accelerate particles up to the TeV regime. The study of gamma-ray emission from novae provides an exceptional real-time laboratory for investigating particle acceleration mechanisms. Unlike supernova remnants, which are large-scale structures, novae present a more compact and transient environment, allowing for detailed temporal observations. However, the presence of multiple shocks within the nova system, including internal shocks within the ejecta and external shocks interacting with the red giant wind,

introduces complexity in understanding the acceleration processes. These observations underscore the potential of novae as laboratories for studying shock dynamics and particle acceleration in astrophysical contexts. The evidence of VHE gamma-ray emission from MGAB-V207 reported by H.E.S.S. [11], making it the first classical nova seen at TeV energies, further challenges existing models. This new result suggests that classical novae can accelerate particles to tens of TeV and that internal shocks may play an essential role in such systems.

3. Gamma-ray emission from historical supernovae

3.1 The case of Kepler

The last Galactic supernova to be observed from Earth occurred on October 9, 1604, and a detailed report was produced by Johannes Kepler, whose name is now attached to the supernova and its remnant. The γ-ray excess as seen with the H.E.S.S. telescopes [14] and with the *Fermi*-LAT [15] is not significantly extended and is fully compatible with the radio, infrared, and X-ray spatial distribution of the SNR. Acero et al. (2022) [15] successfully characterized the multi-wavelength emission with a model in which accelerated particles interact with the dense circumstellar material in the northwest portion of the SNR and radiate GeV γ rays through neutral pion decay. The X-ray synchrotron and inverse-Compton emission mostly stem from the fast shocks in the southern regions with a magnetic field B $\sim$ 100 μG or higher. Depending on the exact magnetic field amplitude, the TeV γ-ray emission could arise from either the southern region (inverse-Compton dominated) or the interaction region in the northwest (pion-decay dominated). In both scenarii, the local proton energy budget is therefore equivalent to about 4% of the local kinetic energy, assuming an energy explosion of 10^{51} erg, much lower than the 10% usually assumed to maintain the CR flux in the Galaxy. We note that if the inverse-Compton emission arises from the fast moving shocks in the southern regions, the precise location of the TeV γ-ray emission might be able to constrain the hadronic or leptonic nature of the emission and, indirectly, the average magnetic field in the SNR. With an increased sensitivity and spatial resolution, the next-generation Cherenkov Telescope Array Observatory [16] will probe Kepler's γ-ray emission spatial distribution with greater accuracy and bring additional constraints on its nature.

3.2 Hadronic emission in the SW rim of SN 1006 ?

Located at a distance of 2.2 kpc [17], the Type Ia supernova remnant SN 1006 was the first SNR in which a non-thermal hard X-ray component was detected in the rim of the remnant by ASCA [18], providing clear evidence of DSA of electrons to high energies in the northeast (NE) and southwest (SW) limbs. Deep very-high-energy (VHE, >100 GeV) observations with the H.E.S.S. array between 2003 and 2008 revealed a bipolar γ-ray morphology closely correlated with the non-thermal X-ray emission [19]. A γ-ray source coincident with SN 1006 was later reported at the 4σ significance level by Xing et al. (2016) using 7 years of LAT data [20]. Using 15 years of *Fermi*-LAT observations and a detailed morphological analysis above 1 GeV, Lemoine-Goumard et al. (2025) [21] detect γ-ray emission from the northeast (NE) rim of SN 1006 at the 6σ level and from the SW rim at the 5.5σ level, employing radio templates from the GLEAM survey. Spectral analysis over the 100 MeV – 1 TeV range yields a hard spectral index of $1.7 \pm 0.1 \pm 0.1$ for the NE

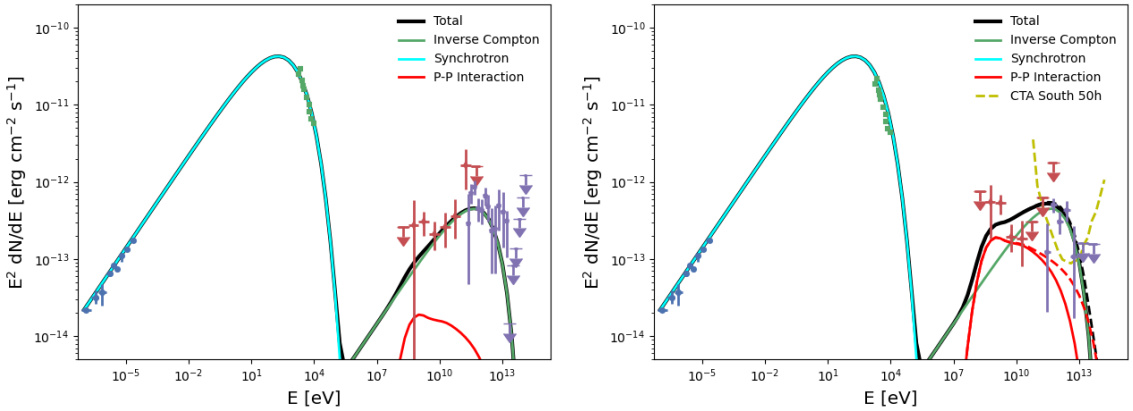

Figure 2: Spectral energy modelling of the NE (Left) and SW (Right) regions of SN 1006. For all experiments except *Fermi*, only statistical errors are shown. The cyan and green lines represent the synchrotron emission and the IC emission, respectively. The black and red dotted lines represent the total and pion decay emission derived for a proton energy cut-off at 200 TeV while the solid ones are derived for 20 TeV. The dashed yellow line indicates the sensitivity of CTAO for 50 hours of observation (latest response function: Southern array Prod 5). The blue radio [22] and green X-ray [23] data from the whole SNR have been scaled for each limb. The H.E.S.S. spectral points for each limb [19] are indicated in purple. The data points derived in this analysis for the NE and SW limbs are presented in red. Modelling parameters and more details in [21].

limb, while the SW emission is characterized by a steeper index of $2.2 \pm 0.1 \pm 0.1$. The authors also report a marginal ($\sim 3\sigma$) detection coincident with the bright northwestern (NW) Hα filament, with a spectral index of ~ 2.1. The broadband non-thermal emission from the NE and SW limbs is well described by a model in which inverse-Compton scattering dominates in the NE, whereas hadronic interactions become increasingly relevant in the SW especially below a few GeV due to the higher ambient density as can be seen in Figure 2. Following this modeling, the total energy transferred to accelerated protons is of the order of 2.6×10^{49} erg. This energy is concentrated in the limbs and would amount to 13% of the kinetic energy, assuming a volume factor of 20% and an explosion energy of 10^{51} erg. This is consistent with the efficient acceleration derived in the limbs by Giuffrida et al. (2022) [24], but also with the value of 4% derived for the whole SNR in the case of the historical supernova Kepler [15].

3.3 Shell-type remnants

Comparing the five most famous shell-type SNRs, we can easily see that all five sources have a hard HE photon index (< 1.8), which suggests a common scenario where the bulk of the emission is produced by accelerated electrons radiating from radio to VHE γ-rays through synchrotron and inverse Compton processes. In addition when correcting for the distance, all SNRs show a surprisingly similar γ-ray luminosity supporting the idea of a common emission mechanism. While the γ-ray emission is likely to be leptonic-dominated at the scale of the whole SNR, this does not rule out efficient hadron acceleration in those objects. This similar γ-ray luminosity was not a priori expected given the fact that our sample is composed of different types of SN explosion and ages ranging from 1 to 6 kyr. Nevertheless, the sources in our sample share an important characteristic that could explain part of this γ-ray similarity. This characteristic is that the SNRs have evolved for

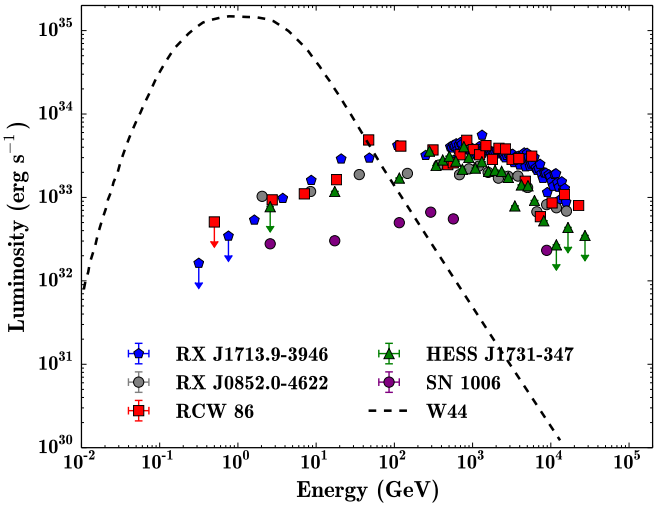

Figure 3: Gamma-ray luminosity of the five shell-type SNRs detected by *Fermi*-LAT and the H.E.S.S. telescopes. For the sake of comparison the SED from the SNR W44 is shown by the dashed line. This Figure was taken from Benjamin Condon's thesis.

most of their life in a low-density ambient medium, which allowed them to maintain a high shock velocity over a long period of time and therefore efficiently accelerate particles to high energies. In this low-density ambient medium, the γ-ray emission is dominated by the leptonic mechanism in which the main source of the photon field, the CMB, is common to all the SNRs. The γ-ray luminosity of SN 1006 is lower than for other SNRs. This is probably related to the SNR bipolar morphology and the reduced surface for efficient particle acceleration. If we correct for this effect by a renormalization factor of 0.2 as discussed in Berezhko et al. (2009) [25], the peak luminosity is comparable to other SNRs. Even if the gamma-ray emission is dominated by leptonic processes, the hadronic process might play a role in some denser sub-regions, as we have seen in the case of SN 1006.

4. Puppis A: a transition case

Puppis A is a SNR adiabatically expanding into the interstellar medium in the vicinity of a large molecular cloud. At an age of only 4500 years [26] implying that the SNR is currently in the Sedov-Taylor evolutionary phase, it is amongst the youngest Galactic SNRs known to be interacting at several locations throughout the shell with dense gas seen as a complex of small HI and CO clouds. This makes Puppis A an interesting transitional case between young SNRs still evolving into a circumstellar medium (e.g. Cas A), and older SNRs which are interacting with large, dense molecular clouds (e.g. IC 443). Using 14 years of *Fermi*-LAT observations, Giuffrida et al. (2025) [27] revealed an asymmetric γ-ray emission shaped by its interaction with the dense molecular cloud in the northeast and a lower-density medium in the southwest. Both regions show spectra consistent with a hadronic origin, though the SW emission is compatible with standard DSA, while

the NE likely involves re-acceleration of pre-existing cosmic rays or reflected shocks. Indeed, the scenario assuming standard DSA on both sides of the remnant faces several challenges: (i) it fails to yield realistic cosmic-ray energies unless the observed shock–cloud interaction [30] is ignored, and (ii) even without accounting for the interaction, it cannot fully explain the observed γ-ray flux differences between the northeastern and southwestern regions based on the X-ray–inferred density contrast. Nevertheless, although less favored, this scenario cannot yet be definitively excluded. The authors also detect two γ-ray excesses outside the remnant, 4FGL J0822.8−4207 and a previously unreported southern source, PS J0824.0−4329, which are both associated with dense interstellar clumps. These dense clumps provide an effective target for production of γ rays. Indeed, high energy particles can escape the remnant, diffuse in the interstellar medium and interact within the cloud via proton-proton interaction, thus producing gamma rays with hard spectra as was originally proposed by Gabici et al. (2009) [28]. This is exactly the properties of these two sources, characterized by a hard spectrum which can be fit by a power law with an index of ~ 2. The energy density of cosmic rays estimated around Puppis A, well above the average in the Galaxy, also points towards an emission originating from CRs escaped from the closely SNR Puppis A and interacting with dense clouds. Another possibility would be that the emission of 4FGL J0822.8−4207 is associated with the young stellar object HH 219 in a local star-forming region [29], but this scenario would fail to explain the southern source.

5. SNR contribution to LHAASO sources : passively illuminated clouds

Particles escape from the remnant and subsequent interaction with nearby dense material, atomic or molecular gas in interstellar clouds, producing gamma rays could contribute to some ultra-high-energy (UHE) LHAASO sources. Indeed, it is puzzling to note that a very small fraction of UHE detected by HAWC and LHAASO are associated with SNRs. One possibility, explored by Mitchell and Celli (2024) [31], is that PeV particles escaped in the early stages of shock evolution. By coupling the modeling of particle escape from known SNRs in a physically motivated framework with molecular cloud environments in the Galaxy, the authors examine the role of SNR-illuminated clouds as potential counterparts to sources listed in the first LHAASO catalog. Their results indicate that such illuminated clouds could account for part of the gamma-ray emission observed from several currently unidentified sources. The best candidate is 1LHAASO J1857+0203u, associated to the unidentified TeV source HESS J1858+020, which is coincident with a molecular cloud that could be illuminated by the SNR G036.6−0.7 under a type II SN scenario (see Figure 4). Nonetheless, further dedicated studies will be required to test and validate the hypothesis of passive UHE gamma-ray sources in the future.

During hadronic processes, neutrinos are also generated, which can serve as a smoking gun for proton acceleration. Interestingly, there is one high-energy starting event (HESE) neutrino observed by the IceCube experiment within the first LHAASO catalog [32]. This event is located in the region of 1LHAASO J1929+1846u which is 0.3° west of SNR G54.1+0.3, and lies within a molecular cloud (see Figure 4 right). SNR G54.1+0.3 was first discovered at a frequency of 4.75 GHz: this radio source was proposed as a Crab-like SNR for its flat spectral index and filled-center morphology. Li et al. (2010) [33] showed that a purely leptonic scenario cannot simultaneously account for the X-ray and gamma-ray observations, whereas a hybrid model combining both leptonic and hadronic

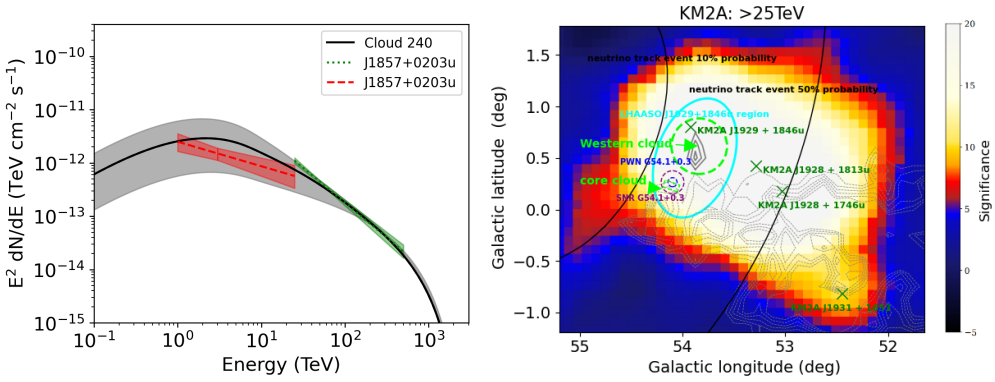

Figure 4: (Left) 1LHAASO J1857+0203u compared to cloud 240 at $(l, b) = (36.10°, -0.14°)$ as derived by [31]. Power law spectra shown with a red dashed or green dotted line correspond to measurements by LHAASO WCDA or KM2A respectively. (Right) Significance map above 25 TeV derived with LHAASO KM2A for the region of 1LHAASO J1929+1846u [34]. The green cross symbol represents the LHAASO source, and the gray dashed line shows the molecular clouds profile. The cyan ellipse roughly represents the WCDA J1929+1846u region, which covers both SNR G54.1+0.3 and the Western Cloud. The light green dotted circle represents the Western Cloud region, and the light green dotted rectangle represents the Core Cloud region. The blue dotted circle indicates the PWN region, and the purple dotted circle indicates the Shell region (Bocchino et al. 2010). Two black solid lines represent the 10% and 50% probability contours of the neutrino event, respectively.

components provides a consistent explanation [33]. G54.1+0.3 is a young remnant with a powerful shell that may still accelerate particles up to PeV energies. In the recent work of Shi et al. (2025) [34], they model the leptonic emission from both the PWN and the SNR shell to reproduce the radio, X-ray, and gamma-ray data, and include an additional hadronic contribution from cosmic rays escaping the remnant to account for the new LHAASO results. This hybrid approach successfully explains the LHAASO observations around the Western Cloud but it requires the SNR G54.1+0.3 to be able to accelerate CRs to PeV. Future observations on this region by CTAO, and by future neutrino telescopes will provide more clues.

6. Middle-aged supernova remnant and interaction with molecular clouds

6.1 Looking for low energy spectral breaks

When accelerated protons encounter interstellar material, they produce neutral pions, which in turn decay into gamma-rays. This offers a compelling way to identify the acceleration sites of protons. A characteristic hadronic spectrum, with a low-energy break around 200 MeV, was detected in the gamma-ray spectra of 2 supernova remnants (SNRs), IC 443 and W44, early in the mission of the Fermi Large Area Telescope [35]. S. Abdollahi et al. (2022) [36] performed a systematic search for low-energy gamma-ray spectral breaks (50 MeV–1 GeV) in 311 *Fermi*-LAT 4FGL sources located near the Galactic plane. They identified 56 objects with statistically significant breaks, including 13 supernova remnants where the spectral shapes are consistent with pion-decay emission (see Figure 5), providing strong evidence for hadronic cosmic-ray acceleration in these environments. Beyond SNRs, the study also revealed characteristic breaks in several binary

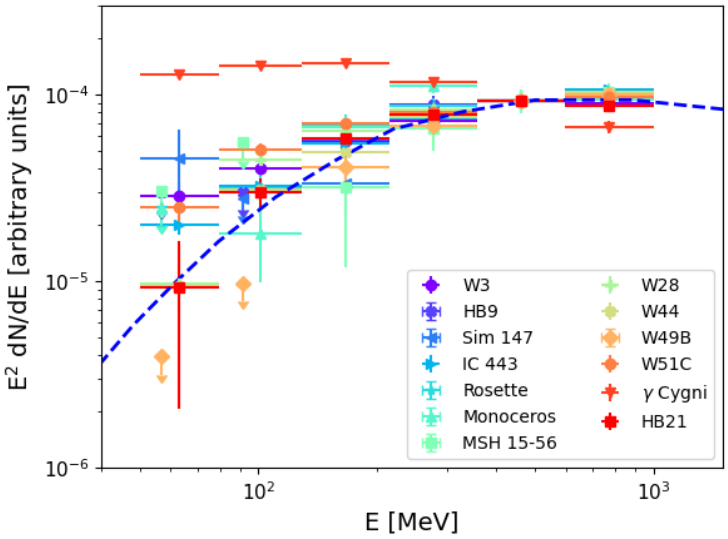

Figure 5: LAT SEDs derived for identified SNRs with significant spectral breaks in [36]. All SEDs have been scaled to the same flux at 500 MeV. The gamma-ray flux produced by a power-law distribution of protons with spectral index of 2.4 as predicted by naima [43] is overlaid in blue.

systems, most notably the high-mass gamma-ray binary LS I +61 303 and the colliding-wind binary Eta Carinae, as well as in the Cygnus star-forming region. These detections highlight that efficient proton acceleration is not limited to SNR shocks, but can also occur in compact binary systems and massive stellar clusters, broadening the range of Galactic accelerators. The results strengthen the case for using low-energy spectral features as robust tracers of hadronic processes across multiple source classes in the Milky Way.

6.2 W51C: acting as a PeVatron ?

Cao et al. (2024) [37] present LHAASO observations of the W51 complex, revealing γ-ray emission extending up to $\sim$ 200 TeV, the first detection of such energies from this region. The spectrum shows a distinct bending at tens of TeV, and when combined with *Fermi*-LAT data—including the pion-decay bump at GeV energies—the broadband emission is well described by hadronic proton-proton interactions. The implied parent proton spectrum features either an exponential cutoff near $\sim$ 400 TeV or a spectral break at $\sim$ 200 TeV. The authors conclude that these results demonstrate that the supernova remnant W51C can accelerate particles close to the PeV domain, positioning it as another Galactic PeVatron candidate. Regarding other potential accelerators within the W51 complex, the authors conclude that the γ-ray contribution from the PWN candidate CXO J192318.5+140305 to the LHAASO observed radiation is marginal. Two young star clusters in W51B (G48.9-0.3 and G49.2-0.3) may be theoretically viable to account for the most energetic γ rays observed by LHAASO, while the relatively coarse angular resolution of LHAASO precludes precise source identification through morphological analysis. The complex interplay of these sources underscores the importance of multi-wavelength and next-generation high-

resolution observations (CTAO, ASTRI Mini-Array, LACT) to disentangle the dominant particle accelerators and to firmly establish the origin of the PeV-scale cosmic rays in this region.

6.3 SNR G106.3+2.7: another PeVatron candidate

SNR G106.3+2.7, also known as the Boomerang region, is another prominent PeVatron candidate in our Galaxy coincident with a molecular cloud. VERITAS first detected extended very-high-energy γ-ray emission, VER J2227+608, which is elongated and offset from the associated pulsar PSR J2229+6114, suggesting the pulsar wind nebula is not the dominant γ-ray source [38]. MAGIC later resolved the emission into head and tail regions, with γ-rays above $\sim$ 6 TeV detected exclusively from the tail [39]. Under the assumption that emissions above 10 TeV detected with air shower experiments (Milagro, HAWC, Tibet ASγ and LHAASO) are emitted only from the SNR tail, the leptonic model for the tail region is in contradiction with the emission above 10 TeV and X-rays. In contrast, the hadronic model could reproduce the observed spectrum at the tail by assuming a proton spectrum with a cutoff energy of 1 PeV. Such high-energy emission in this middle-aged SNR (4-10 kyr) can be explained by considering a scenario where protons escaping from the SNR in the past interact with surrounding dense gases at present. *Fermi*-LAT analysis over 12 years shows a hard GeV–TeV spectrum, further supporting the hadronic origin of the emission of the tail [40]. Together, these observations suggest that G106.3+2.7 is a site of extreme particle acceleration, with the tail acting as the main PeVatron zone. Future high-resolution studies with CTAO and the ASTRI Mini-Array aim to spatially disentangle the head and tail emissions and confirm the maximum proton energies [41]. Overall, G106.3+2.7 exemplifies how multi-instrument observations across GeV–TeV energies can pinpoint potential Galactic PeVatrons.

7. Search for new supernova remnants

7.1 *Fermi* catalogs of extended sources

The first *Fermi* Galactic Extended Source Catalog (FGES), based on six years of Pass 8 data above 10 GeV [42], established the first systematic inventory of extended γ-ray sources in the Galactic plane ($|b| \leq 7^\circ$). It reported 46 extended sources, with detailed morphologies, spectra, and associations. Many of these were linked to known supernova remnants (SNRs) and pulsar wind nebulae (PWNe), providing a reference set of hard-spectrum sources bridging the GeV–TeV regime. Building on this, the Second *Fermi* Galactic Extended Source Catalog (2FGES) [44] analyzed 14 years of LAT data above 10 GeV, focusing on the inner plane ($|l| \leq 100^\circ$, $|b| \leq 1^\circ$). It identified 40 extended sources, nearly half of them newly recognized at GeV energies. Thirteen coincide with established TeV emitters, while several others are associated with bright pulsars, consistent with interpretations in terms of pulsar halos produced by escaping electron/positron pairs. Most sources exhibit hard spectra (photon indices < 2.5) and angular sizes below 1°. Together, these catalogs demonstrate that the GeV extended γ-ray sky along the Galactic plane is dominated by SNR/PWN systems and pulsar halos, with a growing number of direct correspondences to TeV detections. The progression from FGES to 2FGES highlights the role of long-baseline LAT observations in revealing new classes of extended emitters and in constraining the population of Galactic accelerators responsible for high-energy cosmic rays.

A good example is provided by the region of the SNR IC 443, one of the best-studied gamma-ray emitting remnants, interacting strongly with surrounding molecular clouds. At TeV energies, VERITAS mapped gamma-ray emission that correlates perfectly with the gamma-ray emission seen by the LAT, tracing shocked molecular gas, confirming that cosmic rays interact efficiently with dense material [47]. The FGES catalog reported an extended emission exceeding the size of IC 443, namely FGES J0619.6+2229, although it was unclear whether this emission was the result of cosmic rays accelerated by IC 443 diffusing in the surrounding region or originated from a different object such as the SNR candidate G189.6+03.3, discovered in 1994 with ROSAT. More recently, Camilloni & Becker (2023) [45] used data from eROSITA to confirm the SNR of G189.6+3.3 and proposed that the progenitors of G189.6+03.3 and IC 443 could have been expelled from the same binary or multiple system. Re-analysis of the region using 16 years of LAT data by Michailidis et al. (2025) [46] reveals that the gamma-ray emission associated with G189.6+3.3 has two components, one leptonic and the other one hadronic due to proton-proton interaction with the S249 HII cloud with which IC 443 is interacting. These results, confirm that the two remnants evolve at the same distance, and strongly support the binary hypothesis. This would represent the first observation of such an intriguing system.

7.2 Population of radio-dim SNRs at high latitude

The first FGES catalog included another recently discovered SNR G150.3+4.5, characterized by a shell-like morphology with an angular size of 3° in the radio band [49]. Follow-up analysis by Devin et al. (2020) [48] revealed a γ-ray emission spatially coincident with the radio SNR and its hard spectrum with detected photons up to hundreds of GeV suggested that the SNR is dynamically young. Interestingly, this analysis also detected a soft point source (4FGL J0426.5+5434) is located in the southern part of the SNR (see Figure 6 left) with a significance of 25σ between 100 MeV and 1 TeV and a log-parabola spectrum: this source has a pulsar-like spectrum and dominates the low-energy part of the γ-ray emission (E < 3 GeV), while the contribution from the SNR arises at higher energy. The recent LHAASO detection of G150.3+4.5 has revealed this faint radio SNR as a promising new Galactic PeVatron candidate. A detailed analysis with 14 years of *Fermi*-LAT data [50] showed a marked asymmetry between the northern and southern regions of the remnant. The northern lobe exhibits a hard broken power-law spectrum with a break at 150 GeV, consistent with inverse-Compton emission from relativistic electrons in a low-density environment. In contrast, the southern lobe shows a single power-law spectrum that spatially overlaps with molecular material, favoring a hadronic origin from cosmic-ray protons interacting with dense gas. The authors suggest that the LHAASO KM2A detection of a point-like PeV source coincident with this southern region supports the scenario in which escaping CRs illuminate nearby molecular clouds, requiring suppressed diffusion relative to the Galactic average. Another possibility would be that the emission detected by LHAASO KM2A is related to a putative PWN associated with the point source 4FGL J0426.5+5434. Future observations on this region by CTAO but also with radio telescopes would prove extremely useful to constrain the origin of this new PeV source.

This SNR is a cornerstone example of a full population of radio-dim but γ-ray–bright SNRs that complement the classical radio-bright shell remnants. Comparable behaviour has been identified in G279.0+1.1 [51], which shows extended hard GeV emission ($\Gamma \approx 1.9$) roughly coincident with its radio shell. G17.8+16.7 [52] also presents nonthermal radio and GeV emission consistent with a

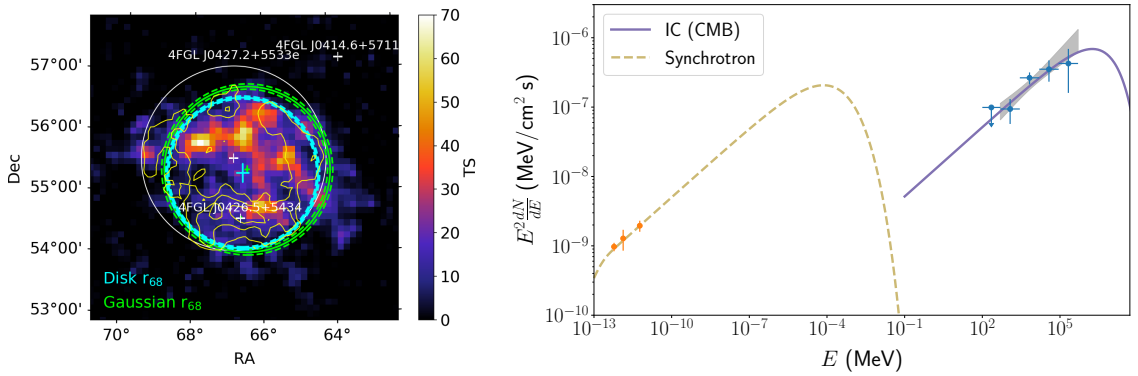

Figure 6: (Left) TS map of SNR G150.3+4.5 obtained from 1 GeV to 3 TeV without 4FGL J0426.5+5434 included in the model. The best-fit Gaussian and disk are represented in green and blue, respectively. The crosses are the centroid uncertainties (1σ), while the solid and dashed circles correspond to the r_{68} with its associated statistical errors (1σ). The 4FGL sources are shown in white and the Urumqi 6 cm radio contours (at 6, 11, and 16 mK T_B) are overlaid in yellow. (Right) Non thermal fluxes measured from SNR G118.4+37.0 as derived by [54]. The radio data were obtained from [55]. The GeV fluxes from this work are shown with their 1σ statistical uncertainties. A 95%-confidence level upper limit is shown for the energy interval 100–500 MeV. The dashed and solid lines represent the leptonic emission model applied to the data. The gray band represents the 1σ propagated statistical uncertainty from the fit to the LAT data in the entire energy range used.

shell-type SNR. At higher latitude, G118.4+37.0 [53, 54]) exhibits faint radio emission but bright, hard GeV γ-rays (Figure 6 right) that can be explained by inverse-Compton emission in a low-density environment. Similarly, G288.8−6.3 (Ancora) [56] combines a faint radio shell with extended GeV emission correlated with brighter arcs, again favoring leptonic interpretations. Collectively, these remnants share hard GeV spectra ($\Gamma \leq 2.1$), low radio surface brightness, and relatively isolated or low-density environments, pointing to efficient particle acceleration even in evolved or faint shells. They illustrate that γ-ray observations can uncover SNRs invisible or inconspicuous in radio surveys, expanding the known population of Galactic CR accelerators.

At the same time, three γ-ray–bright SNRs at high latitude—G310.7−5.4 (Burger-Scheidlin 2025 [57]), HB21 [58], and G166.6+4.3 [59] —show softer GeV spectra ($\Gamma \geq 2.5$), likely reflecting differences in age, particle transport or in environment, the key ingredient governing the evolution of SNR shocks and their subsequent gamma-ray emissions. Together, these studies highlight the diversity of γ-ray SNRs beyond the classical radio-bright population, revealing a new class of radio-faint but γ-ray–luminous remnants that expand our view of Galactic cosmic-ray accelerators.

7.3 Non-detections within the H.E.S.S. Galactic Plane Survey

Non-detections can also provides strong constraints in some cases. In a recent study, Brun et al. (2025) [60] have used the FITS maps of flux upper limits along the Galactic plane released with the H.E.S.S. Galactic Plane Survey (HGPS; [61]) and compared them with extrapolated *Fermi*-LAT spectra from the 4FGL-DR3 catalog. This analysis revealed several sources where the extrapolated *Fermi* flux exceeds the H.E.S.S. constraints. The authors highlight four such cases: 4FGL J1712.9−4105, 4FGL J1735.9−3342, 4FGL J1830.1−1440, and 4FGL J1830.3−1601. The

latter two are spatially coincident with the supernova remnants (SNRs) G354.8−0.8 and G016.2−0.7, respectively, while the others lack clear associations. For SNR G354.8−0.8, the *Fermi*-LAT source lies near the center of the radio shell and exhibits a hard spectrum (1.67 ± 0.16). The detection of OH (1720 MHz) maser emission indicates shock–cloud interaction, favoring a hadronic origin of the γ rays. However, the hard spectrum is more naturally explained by leptonic inverse-Compton emission, unless hadronic models involving dense gas clumps are invoked.

8. Future prospects

8.1 The population of remnants as seen by CTAO

The Cherenkov Telescope Array Observatory (CTAO) is the next-generation ground-based gamma-ray observatory, with arrays in both the Northern and Southern Hemispheres. It will cover an energy range from $\sim$ 20 GeV to $>$ 300 TeV, combining excellent angular and energy resolution with improved sensitivity. One Large-Sized Telescope (LST) is already operational in the Northern array, and three more are expected to be operational in 2026. CTAO features telescopes of different sizes (LST, MST, SST) to optimize coverage of both low- and high-energy gamma rays, and its larger fields of view, especially for MSTs and SSTs, will alleviate the small-FOV limitation of current Cherenkov arrays. It will provide detailed imaging and spectroscopy of supernova remnants, complementing wide-field instruments like HAWC and LHAASO. Batzofin et al. (2024) [62] presents a detailed analysis of the Galactic SNR population observable in the TeV gamma-ray regime. Through Monte Carlo simulations, the authors model the distribution and characteristics of SNRs, comparing their findings with existing data from the H.E.S.S. Galactic Plane Survey. The study provides insights into the acceleration mechanisms at play within SNRs, including the balance between hadronic and leptonic processes. These simulations serve as a benchmark for interpreting future observations from the CTAO's GPS, offering a predictive framework for understanding the TeV emission from SNRs and their contribution to the broader cosmic-ray spectrum. The combination of the CTAO's upcoming Galactic Plane Survey [63] and the detailed population models provided by Batzofin et al. sets the stage for a transformative era in SNR research. By leveraging the high sensitivity and extensive coverage of the CTAO, one can anticipate that a vast number of previously undetected SNRs will be uncovered, including those that are faint or obscured in other wavelengths. Indeed, SNRs correspond to the second-most numerous class detected in the GPS. About half of the synthetic SNRs detected are significantly spatially extended, which is a valuable feature for the identification of sources with multi-wavelength counterparts. The distribution of SNRs in integral true simulated flux and distance in Figure 7 shows that new sources can be detected out to the other side of our Galaxy. The newly detected shell-type SNRs have an age range from 0-10 kyrs with a detection efficiency of 15-30% in each age bin and an average of 3 SNRs per 1 kyr age bin. This wider distribution of ages than current samples will pave the way to a more detailed population study. This comprehensive mapping will not only enhance our understanding of SNRs as cosmic-ray accelerators but also shed light on their evolution, interaction with the interstellar medium, and their role in the Galactic ecosystem.

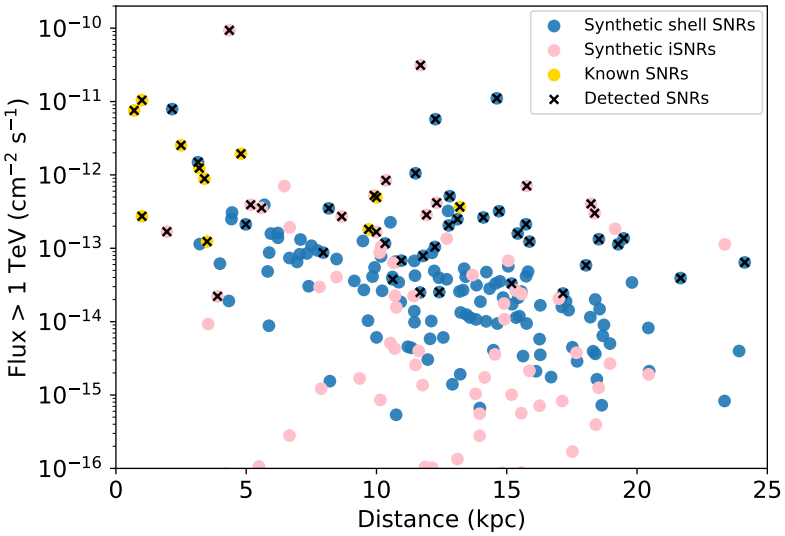

Figure 7: Comparison of the known SNRs and the population of synthetic shell and interacting SNRs in the integral true simulated flux-distance parameter space, as derived in [63]. New objects can be detected up to a distance of 20 kpc and down to an integral flux of a few 10^{-14} cm^{-2} s^{-1}. Note that for a given flux, the detectability of a SNR depends on its extension.

8.2 Complementary on-going constructions or developments

Besides CTAO, three other instruments are currently in development. First, the ASTRI (Astrofisica con Specchi a Tecnologia Replicante Italiana) Mini-Array is an array of nine dual-mirror Cherenkov telescopes under construction at the Teide Astronomical Observatory in Tenerife, Spain [64]. It aims to operate in the energy range of 1–300 TeV, providing high angular resolution and sensitivity. ASTRI's design allows for precise imaging of extended sources, making it an ideal instrument for follow-up observations of SNRs detected by other observatories. Second, the Large Array of Cherenkov Telescopes (LACT) is an array of imaging atmospheric Cherenkov telescopes being constructed by LHAASO at the 4410 m altitude site in Sichuan Province, China [65]. The array is designed to operate in the very-high-energy (VHE) and ultra-high-energy (UHE) gamma-ray regimes, providing high angular resolution and sensitivity. The array's construction is expected to be completed by 2028, and it will significantly contribute to the study of SNRs and other high-energy astrophysical sources. Third, the Southern Wide-field Gamma-ray Observatory (SWGO) is poised to significantly enhance our understanding of cosmic-ray accelerators in the Southern Hemisphere [66]. Though, its development is less advanced than the two others, with its strategic location in the Southern Hemisphere, SWGO will provide optimal coverage of regions such as the Galactic Center (GC), which is challenging to observe from Northern Hemisphere facilities. Its wide field of view ($\sim$ 2 steradians) and high duty cycle ($\sim$ 95%) make it particularly suited for monitoring extended sources and transient events. SWGO's sensitivity extends up to several hundred TeV, enabling the detection of ultra-high-energy (UHE) gamma-ray emissions from SNRs. This capability is crucial for identifying potential hadronic PeVatrons—astrophysical accelerators capable of accelerating protons to energies exceeding 10^{15} eV. The observatory's large field of view allows for efficient monitoring of extended sources, such as star-forming regions and massive stellar clusters, which

are often associated with SNRs.

9. Conclusions

Gamma-ray observations have revealed a remarkable diversity among Galactic supernova remnants in terms of age, evolutionary stage, and ambient environment. Young remnants, such as G106.3+2.7 and G150.3+4.5, often exhibit hard spectra and high-energy emission, suggesting efficient particle acceleration early in their evolution. Older remnants, like W51C and HB21, show softer spectra and interaction with molecular clouds, highlighting the influence of environmental density on gamma-ray production. Importantly, gamma-ray observations have proven to be a particularly powerful tool for detecting radio-dim remnants, which are often missed in radio surveys but contribute significantly to the Galactic SNR population. The diversity of gamma-ray SNRs indicates that particle acceleration efficiency depends not only on age but also on local conditions, especially the surrounding gas density. Some remnants interacting with dense molecular clouds produce enhanced gamma-ray flux through hadronic interactions, providing unique laboratories to study cosmic-ray propagation and interactions. Despite extensive studies across GeV–TeV energies, no SNR has yet been firmly identified as a PeVatron, capable of accelerating protons to the knee of the cosmic-ray spectrum. However, evidence from sources like 1LHAASO J1929+1846u, W51C, and G106.3+2.7 suggests that the escape of high-energy protons at early evolutionary stages may play a critical role in seeding the interstellar medium with cosmic rays.

Beyond SNRs, other potential Galactic accelerators such as microquasars, pulsar wind nebulae, and massive stellar clusters may contribute significantly to the cosmic-ray budget, highlighting the need for a multi-source approach to understanding acceleration. Future gamma-ray facilities, particularly CTAO, LHAASO, and the upcoming SWGO, will be crucial to probe the highest-energy emission, resolve spatially complex regions, and detect faint or radio-dim remnants. Such observations will clarify the role of early escape in shaping the cosmic-ray spectrum and may identify hidden PeVatron candidates in collective or isolated environments. Overall, gamma-ray astronomy is increasingly revealing the complex interplay between SNR evolution, environment, and particle acceleration, emphasizing that cosmic-ray production in the Galaxy likely involves both individual remnants and collective processes. Continued observations promise to refine our understanding of the sources, mechanisms, and propagation of high-energy cosmic rays, bringing us closer to resolving one of astrophysics' long-standing puzzles.

The emerging multi-messenger landscape also invites a broader view of cosmic-ray acceleration beyond isolated remnants. The detection of PeV photons from G106.3+2.7 and tentative neutrino associations highlight the potential of joint γ–ν analyses to directly trace hadronic acceleration. Future cross-correlation of *Fermi*, CTAO, LHAASO, and IceCube/KM3NeT observations will critically test whether hadronic interactions in SNR shocks can produce measurable neutrino fluxes. At the same time, collective acceleration in superbubbles, OB associations, and stellar clusters may offer a complementary—or even dominant—pathway to the Galactic PeVatron population. The interplay of multiple shocks, turbulence driven by stellar winds, and large-scale magnetic loops can sustain acceleration to several PeV over extended timescales [67], as suggested by the γ-ray emission from the Cygnus Cocoon [68, 69] and Westerlund 1 [68, 70, 71].

Acknowledgement

I would like to thank the ICRC 2025 organizers for their kind invitation to present these results. I would also like to thank my collaborators from the H.E.S.S. and *Fermi*-LAT collaborations for useful discussion.

References

[1] Baade, W. & Zwicky, F. 1934, Proceedings of the National Academy of Science, 20, 5, 259. doi:10.1073/pnas.20.5.259

[2] Bell, A. R. 1978, MNRAS, 182, 147. doi:10.1093/mnras/182.2.147

[3] Bell, A. R., Schure, K. M., Reville, B., & Giacinti, G. 2013, MNRAS, 431, 415, doi:10.1093/mnras/stt179

[4] Caprioli, D. 2015, 34th International Cosmic Ray Conference (ICRC2015), 34, 8. doi:10.22323/1.236.0008

[5] Cristofari, P., Blasi, P., & Amato, E. 2020, Astroparticle Physics, 123, 102492. doi:10.1016/j.astropartphys.2020.102492

[6] Diesing, R. 2023, ApJ, 958, 1, 3. doi:10.3847/1538-4357/ad00b1

[7] Marcowith, A., Dwarkadas, V. V., Renaud, M., et al. 2018, MNRAS, 479, 4, 4470. doi:10.1093/mnras/sty1743

[8] H. E. S. S. Collaboration, Aharonian, F., Ait Benkhali, F., et al. 2022, Science, 376, 6588, 77. doi:10.1126/science.abn0567

[9] Acciari, V. A., Ansoldi, S., Antonelli, L. A., et al. 2022, Nature Astronomy, 6, 689. doi:10.1038/s41550-022-01640-z

[10] Abe, K., Abe, S., Abhishek, A., et al. 2025, A&A, 695, A152. doi:10.1051/0004-6361/202452447

[11] Fauverge, P., Mitchell, A., Schussler, F., Mackey, J., Lemoine-Goumard, M., Grondin, M.-H., Tsirou, M., 2025, 39th International Cosmic Ray Conference (ICRC 2025)

[12] Li, S., Liang, Y.-F., Liao, N.-H., et al. 2024, arXiv:2407.05968. doi:10.48550/arXiv.2407.05968

[13] Acero, F., Marti-Devesa, G., 2025, 39th International Cosmic Ray Conference (ICRC 2025)

[14] H. E. S. S. Collaboration, Aharonian, F., Ait Benkhali, F., et al. 2022, A&A, 662, A65. doi:10.1051/0004-6361/202243096

[15] Acero, F., Lemoine-Goumard, M., & Ballet, J. 2022, A&A, 660, A129. doi:10.1051/0004-6361/202142200

[16] Cherenkov Telescope Array Consortium, Acharya, B. S., Agudo, I., et al. 2019, . doi:10.1142/10986

[17] Winkler, P. F., Gupta, G., & Long, K. S. 2003, ApJ, 585, 1, 324. doi:10.1086/345985

[18] Koyama, K., Petre, R., Gotthelf, E. V., et al. 1995, Nature, 378, 6554, 255. doi:10.1038/378255a0

[19] Acero, F., Aharonian, F., Akhperjanian, A. G., et al. 2010, A&A, 516, A62. doi:10.1051/0004-6361/200913916

[20] Xing, Y., Wang, Z., Zhang, X., et al. 2016, ApJ, 823, 1, 44. doi:10.3847/0004-637X/823/1/44

[21] Lemoine-Goumard, M., Acero, F., Ballet, J., et al. 2025, A&A, 693, A193. doi:10.1051/0004-6361/202451944

[22] Allen, G. E., Petre, R., & Gotthelf, E. V. 2001, ApJ, 558, 2, 739. doi:10.1086/322470

[23] Bamba, A., Fukazawa, Y., Hiraga, J. S., et al. 2008, PASJ, 60, S153. doi:10.1093/pasj/60.sp1.S153

[24] Giuffrida, R., Miceli, M., Caprioli, D., et al. 2022, Nature Communications, 13, 5098. doi:10.1038/s41467-022-32781-4

[25] Berezhko, E. G., Ksenofontov, L. T., & Völk, H. J. 2009, A&A, 505, 1, 169. doi:10.1051/0004-6361/200911948

[26] Becker, W., Prinz, T., Winkler, P. F., et al. 2012, ApJ, 755, 2, 141. doi:10.1088/0004-637X/755/2/141

[27] Giuffrida, R., Lemoine-Goumard, M., Miceli, M., et al. 2025, , arXiv:2507.11208. doi:10.48550/arXiv.2507.11208

[28] Gabici, S., Aharonian, F. A., & Casanova, S. 2009, MNRAS, 396, 3, 1629. doi:10.1111/j.1365-2966.2009.14832.x

[29] Araya, M., Gutiérrez, L., & Kerby, S. 2022, MNRAS, 510, 2, 2277. doi:10.1093/mnras/stab3340

[30] Aruga, M., Sano, H., Fukui, Y., et al. 2022, ApJ, 938, 2, 94. doi:10.3847/1538-4357/ac90c6

[31] Mitchell, A. M. W. & Celli, S. 2024, Journal of High Energy Astrophysics, 44, 340. doi:10.1016/j.jheap.2024.10.011

[32] Cao, Z., Aharonian, F., An, Q., et al. 2024, ApJS, 271, 1, 25. doi:10.3847/1538-4365/acfd29

[33] Li, H., Chen, Y., & Zhang, L. 2010, MNRAS, 408, 1, L80. doi:10.1111/j.1745-3933.2010.00934.x

[34] Shi, Y., Cui, Y., & Yang, L. 2025, ApJ, 984, 2, 199. doi:10.3847/1538-4357/adc9a7

[35] Ackermann, M., Ajello, M., Allafort, A., et al. 2013, Science, 339, 6121, 807. doi:10.1126/science.1231160

[36] Abdollahi, S., Acero, F., Ackermann, M., et al. 2022, ApJ, 933, 2, 204. doi:10.3847/1538-4357/ac704f

[37] Cao, Z., Aharonian, F., Axikegu, et al. 2024, Science Bulletin, 69, 18, 2833. doi:10.1016/j.scib.2024.07.017

[38] Acciari, V. A., Aliu, E., Arlen, T., et al. 2009, ApJ, 703, 1, L6. doi:10.1088/0004-637X/703/1/L6

[39] MAGIC Collaboration, Abe, H., Abe, S., et al. 2023, A&A, 671, A12. doi:10.1051/0004-6361/202244931

[40] Fang, K., Kerr, M., Blandford, R., et al. 2022, Phys. Rev. Lett., 129, 7, 071101. doi:10.1103/PhysRevLett.129.071101

[41] Carrasco, M.-S., Cassol, F., Costantini, H., et al. 2024, SF2A-2024: Proceedings of the Annual meeting of the French Society of Astronomy and Astrophysics, 223.

[42] Ackermann, M., Ajello, M., Baldini, L., et al. 2017, ApJ, 843, 2, 139. doi:10.3847/1538-4357/aa775a

[43] Zabalza, V. 2015, 34th International Cosmic Ray Conference (ICRC2015), 34, 922. doi:10.22323/1.236.0922

[44] Abdollahi, S., Acero, F., Acharyya, A., et al. 2024, , arXiv:2411.07162. doi:10.48550/arXiv.2411.07162

[45] Camilloni, F. & Becker, W. 2023, A&A, 680, A83. doi:10.1051/0004-6361/202347300

[46] Michailidis, M., Lemoine-Goumard, M., Wilcox, R., Gabici, S., Di Lalla, N., Omodei, N., 2025, Nature Communications, submitted

[47] Humensky, B., VERITAS Collaboration, & Fermi-Lat Collaboration 2025, AAS, 245, 322.03.

[48] Devin, J., Lemoine-Goumard, M., Grondin, M.-H., et al. 2020, A&A, 643, A28. doi:10.1051/0004-6361/202038503

[49] Gao, X. Y. & Han, J. L. 2014, A&A, 567, A59. doi:10.1051/0004-6361/201424128

[50] Li, Y., Liu, S., & Giacinti, G. 2024, A&A, 689, A257. doi:10.1051/0004-6361/202348873

[51] Araya, M. 2020, MNRAS, 492, 4, 5980. doi:10.1093/mnras/staa244

[52] Araya, M., Hurley-Walker, N., & Quirós-Araya, S. 2022, MNRAS, 510, 2, 2920. doi:10.1093/mnras/stab3550

[53] Xin, Y. & Guo, X. 2022, ApJ, 941, 2, 194. doi:10.3847/1538-4357/aca473

[54] Araya, M. 2023, MNRAS, 518, 3, 4132. doi:10.1093/mnras/stac3337

[55] Arias, M., Botteon, A., Bassa, C. G., et al. 2022, A&A, 667, A71. doi:10.1051/0004-6361/202244369

[56] Burger-Scheidlin, C., Brose, R., Mackey, J., et al. 2024, A&A, 684, A150. doi:10.1051/0004-6361/202348348

[57] Burger-Scheidlin, C., Ball, B. D., Lazarevic, S., et al. 2025, 39th International Cosmic Ray Conference (ICRC 2025)

[58] Pivato, G., Hewitt, J. W., Tibaldo, L., et al. 2013, ApJ, 779, 2, 179. doi:10.1088/0004-637X/779/2/179

[59] Araya, M. 2013, MNRAS, 434, 3, 2202. doi:10.1093/mnras/stt1162

[60] Brun, F., Le Nagat-Neher, B., Lemoine-Goumard M., Grondin, M.-H., Fauverge, P., 2025, 39th International Cosmic Ray Conference (ICRC 2025)

[61] H. E. S. S. Collaboration, Abdalla, H., Abramowski, A., et al. 2018, VizieR Online Data Catalog, 361. doi:10.26093/cds/vizier.36120001

[62] Batzofin, R., Cristofari, P., Egberts, K., et al. 2024, A&A, 687, A279. doi:10.1051/0004-6361/202449779

[63] Abe, S., Abhir, J., Abhishek, A., et al. 2024, J. Cosmology Astropart. Phys., 2024, 10, 081. doi:10.1088/1475-7516/2024/10/081

[64] Vercellone, S. 2024, Universe, 10, 2, 94. doi:10.3390/universe10020094

[65] Zhang, Z., Yang, R., & Zhang, S. 2025, , arXiv:2509.20694. doi:10.48550/arXiv.2509.20694

[66] SWGO Collaboration, Abreu, P., Alfaro, R., et al. 2025, , arXiv:2506.01786. doi:10.48550/arXiv.2506.01786

[67] Vieu, T., Reville, B., & Aharonian, F. 2022, MNRAS, 515, 2, 2256. doi:10.1093/mnras/stac1901

[68] Ackermann, M., Ajello, M., Allafort, A., et al. 2011, Science, 334, 6059, 1103. doi:10.1126/science.1210311

[69] LHAASO Collaboration 2024, Science Bulletin, 69, 4, 449. doi:10.1016/j.scib.2023.12.040

[70] Aharonian, F., Ashkar, H., Backes, M., et al. 2022, A&A, 666, A124. doi:10.1051/0004-6361/202244323

[71] Lemoine-Goumard, M., Härer, L., Mohrmann, L., et al. 2025, Nature Communications, accepted